Structural Analysis of Historical Constructions – Jerzy Jasieńko (ed)
© 2012 DWE, Wrocław, Poland, ISSN 0860-2395, ISBN 978-83-7125-216-7

MECHANICAL ANALYSIS OF AN OLD MASONRY BRIDGE IN PARIS

Nathalie Domède[1], *Thomas Stablon*[2], *Alain Sellier*[3]

ABSTRACT

This communication presents a methodology developed to assess the mechanical behaviour of historical constructions. It is applied to an old masonry bridge close to Paris, built in 1904. This method uses a calculation tool based on a 3D damage model implemented in a FEM code. The model uses homogenized parameters considering masonry heterogeneities. The computing part is preceded by a phase of research on archival documents, an on-site investigation phase, and an experimental phase carried out on core samples in the laboratory. This last phase determines the parameters involved in the homogenized mechanical behaviour law of the masonry. The model is based on the theory of distributed anisotropic cracking. It considers crack-reclosing processes and the possibility of using pre-damage of the material. The latter ability explains the role of crack opening and crack reclosing in the actual stiffness of the structure. The crack opening is supplied by the model and facilitates the assessment of the actual state of the structure from the crack opening measured on the bridge. Once the actual state has been identified, the calculation tool is able to determine the crack pattern induced in the bridge by the loads and other actions, such as displacements of additional supports. This research demonstrates the importance of considering the whole history of a structure in order to assess its current state and supplies a methodology for doing so.

Keywords: *Masonry bridge, Homogenization method, Damage model, Cracking, FEM*

1. INTRODUCTION

This article presents the methodology developed at the University of Toulouse (France) for assessing old masonry arch bridges. This research was supported by the Société Nationale des Chemins de Fer and Réseau Ferré de France, the French railway network. The aim was to develop a global method able to determine the serviceability of masonry railway bridges and to optimize the strengthening that could be needed.
The global bridge population in Europe includes a high proportion of masonry arches, especially on the railway network (60% according to Orban in 2005 (Orban [1]). These bridges are old (more than a hundred years old), traffic is increasing and disorders, cracks, and sometimes collapse, occur. That is why research programmes have been developed (the history of the calculation of masonry bridges is described in Proske and Van Gerlder [2]). They use various approaches: limit analysis, plastic or damage analysis with a macro or micro approach. A review of the methods applicable to the study of historical masonry constructions is given in P. Roca [3]. At the University of Toulouse, works on the behaviour of masonry arch bridges focuses on the emergence of cracking, the determination of the displacements of the structure and of its damaged zones. The final aim is to assess the current behaviour under service loads and to forecast the ultimate loads. The work presented here concerns a long multispan stone masonry bridge.Because the problem is to study full-scale masonry structures with large dimensions, a macro analysis using a homogenized model is employed. It considers the elastic and inelastic domains. In the research presented here, the mechanical behaviour of the masonry

[1] Associate professor, Université de Toulouse; UPS, INSA; LMDC (Laboratoire Matériaux et Durabilité des Constructions) France, nathalie.domede@insa-toulouse.fr
[2] Doctor, thomas.stablon@etud.insa-toulouse.fr
[3] Professor, alain.sellier@insa-toulouse.fr

is described using a continuum damage model. With this model, initially developed by Sellier [4] for concrete, and adapted for masonry, the cracks can appear anywhere in the bridge and go in any direction, in both tensile and compressive zones, then possibly reclose, according to the strain state. The efficiency of this model to describe masonry mechanical behaviour was presented at SAHC 2010 (Domede [5]). Since then, improvements have been made, particularly concerning the crack reclosing management, as will be described later. The current behaviour of the masonry is partially assessed by means of laboratory tests done on samples and is completed by a homogenization method and block-mortar interface pre-damage. But, because of the major influence of existing cracks in the structure, the global mechanical behaviour of an old bridge is strongly dependent on its history (initial building process and subsequent movement of the base, which governs its current stiffness (Stablon [6]). To assess this aspect, we carried out investigations on the bridge in question: measurements of crack openings and vault displacements under train loads. The comparison between relevant values and results of calculations was used to fit the base movements explaining the crack pattern and the current masonry stiffness. A realistic calculation of the bridge was then possible, under service and ultimate loads.

2. THE MECHANICAL BEHAVIOUR MODEL

The approach is a "macro" one regarding the healthy masonry as a homogeneous material. This section presents the continuum orthotropic damage model used, introduced in an FEM code to describe the cracking of this homogeneous masonry.

2.1. Presentation of the model

The model is a variant of the initial concrete model described in detail by Sellier and Bary [4] and completed in 2010 to consider the possibility of crack re-closure. It uses a Rankine multi-criterion in tension and a Drucker Prager criterion in compression. With this 3D damage model, the beginning of cracking and the width of crack opening is determined according to local strain, without any initial assumption on crack location or orientation. The cracks and damage zones are the natural consequences of the localization process induced by the softening phase of the behaviour law.
At the beginning of the loading, the effective stress (σ_{eff}), is calculated according to (1):

$$\left(\sigma_{eff}\right) = C_0\left(\varepsilon_e\right) \tag{1}$$

where: (ε_e) = elastic strain, C_0 = healthy material stiffness matrix (un-cracked).
Then, this effective stress (σ_{eff}) is separated into a negative part (σ_c) in compression and a positive part (σ_t) in tension. The internal variables that characterize the damage state of the masonry are D_c in the compressive domain and D_t in tension. In compression, the negative part (σ_c) is used to assess a Drucker Prager equivalent stress (2), on which the damage variable D_c depends.

$$\sigma_{DP} = \sqrt{\frac{J_{2d}}{6}} + \delta\frac{I_1}{3} \tag{2}$$

where: J_{2d} = second invariant of the deviator of (σ_c), I1 = trace of (σ_c), δ = the Drucker Prager constant, which depends on the internal friction angle φ as follows in (3). δ is determined by experimental tests on samples.

$$\delta = \frac{2\sqrt{3}\sin\varphi}{3-\sin\varphi} \tag{3}$$

In tension, a Rankine Criterion (Maximal Tensile Stress criterion, also called MTS by Erdogan and Sih [7] is used to assess the tensile damage tensor D_t. It affects the effective stress in tension (σ_t), so as to include the crack re-closure phenomenon in the mechanical behaviour of the masonry. The apparent stress to be used at integration points of the finite element code is obtained by (4), where I is the identity tensor.

$$(\sigma) = (I - D_c)\left[(I - D_t)(\sigma_{eff}) + D_t \underbrace{(\sigma_{eff} - \sigma_p)}_{\sigma_{ft}} \right] \quad (4)$$

In equation (4), (σ_p) is a plastic stress following a crack re-closure yield function described in Stablon's work [6]. It is equal to (σ_{eff}) during the damage process, such that the stress in the localized cracks (σ_{ft}) stays equal to zero until a crack re-closure is activated. The behaviour law of the sound material in uniaxial loading is represented on Figure 1. On this figure, the strengths are noted f_c in compression and f_t in tension, and the peak strain in compression is $\varepsilon_{c,peak}$. Before damage, the law is characterized by the same elastic modulus in uniaxial compression and tension, noted E. These 4 parameters (f_c, f_t, E, $\varepsilon_{c,peak}$) have to be determined experimentally. The peak strain in tension $\varepsilon_{t,peak}$ is given by (5) :

$$\varepsilon_{t,peak} = \frac{f_t}{E} \quad (5)$$

As illustrated on Figure 1, the damage leads to a post-peak softening phase in relation with the fracture energy in tension G_{ft} and in compression G_{fc}. To avoid a dependence of the finite element solution on the mesh size, the damage evolution law has to depend on the finite element size. For this purpose, a volumic cracking energy "g_{ft}" (or "g_{fc}") is used (Equations (6) and (7)), depending on the orientation of the crack, and chosen in such a way that the energy under the tensile curve equals G_{ft} (or G_{fc}) whatever the size of the element in the direction perpendicular to the crack.

$$G_{ft} = g_{ft} \times l_m \quad (6)$$

$$g_{ft} = \frac{f_t^2}{2E} + \int_{\varepsilon_{t,peak}}^{\varepsilon_{tR}} E(1 - D_t)\varepsilon d\varepsilon \quad (7)$$

where: lm is the finite element length in the direction perpendicular to the crack.
A method has been developed to determine the length of the finite element perpendicularly to the crack, i.e. in the main stress direction, and the tensile energy dissipated in that direction (Stablon [6]). Finally, the softening phase of the behaviour law depends on the finite element size in an anisotropic way, thus ensuring that the global response of the FEM will be independent of the mesh. This technique allows the structure to be meshed independently of the forecasted cracking pattern.
The model also allows a variable to be plotted that is very interesting for practitioners: the Crack Mouth Opening Displacement (CMOD). It can be calculated directly at the Gauss point during the finite element solving procedure, or post-treated at the end of the whole calculation for each step. CMOD depends not only on the damage state but also on the strain state. In the present modelling, it corresponds to the average crack opening displacement computed assuming a single localized crack in each element damaged in tension. It is approached using (8) in a main direction of the Rankine effective stress.

$$CMOD_m = l_m.(\varepsilon_e).\left[\frac{D_{tm} - D_{t,peak}}{I - D_{t,peak}} \right].H(\sigma_{Rm} - f_t).H\left(\frac{D_{tm} - D_{t,peak}}{I - D_{t,peak}} \right) \quad (8)$$

where: l_m = finite element length in the main direction of cracking "m"; D_{tm} = Tensile damage value in the corresponding main direction 'm'; $D_{t,peak}$ = Damage value at peak in tension (point 1 in Figure 1); σ_{Rm} = Current value of the Rankine criterion in the direction 'm'; H(X) = Heaviside function defined by H(X) = I for X > 0, 0 otherwise.
An illustration of the advantage of using this variable instead of the classic damage variable is the fact that, even if many limited cracks occur in a massive structure, only the main cracks will stay open until failure, and all the surrounding ones will be reclosed. CMOD is then able to capture this main crack among the multiple damaged elements.

2.2. Pre-damage

To approach the current masonry stiffness, and especially the initial brittle state of the mortar-block interface, initial damage of the masonry can be used. Actually, laboratory tests have shown that, for masonry, the stiffness in tension and the stiffness in compression are different. Furthermore, at the very beginning of the loading, the experimental curves in compression show a progressive increase of the stiffness until the Young modulus E is reached. This phenomenon comes from the fact that the material contains micro initial cracks that reclose in compression. In addition, in masonry structures, the shrinkage of the mortar joints between the stones, at construction time, creates pores and cavities that influence the stiffness of masonry, as demonstrated by Stablon [8]. These experimental results are considered in the model by means of a "pre-damage" parameter D_{t0}, transforming the behaviour law of the sound material into a pre-damaged material behaviour law, as illustrated in Figure 1.

Finally, the damage model proposed for the masonry requires 9 parameters that have to be determined initially by experimental tests in the laboratory and a homogenization method: elastic modulus E, Poisson's ratio ν, compressive strength fc and strain at peak in compression $\varepsilon_{c,peak}$, tensile strength f_t, the fracture energy in tension and compression G_{fc} and G_{ft}, the Drucker Prager parameter δ, and the initial damage in tension D_{t0} that allows a pre-existing crack or any localized disorder to be taken into account.

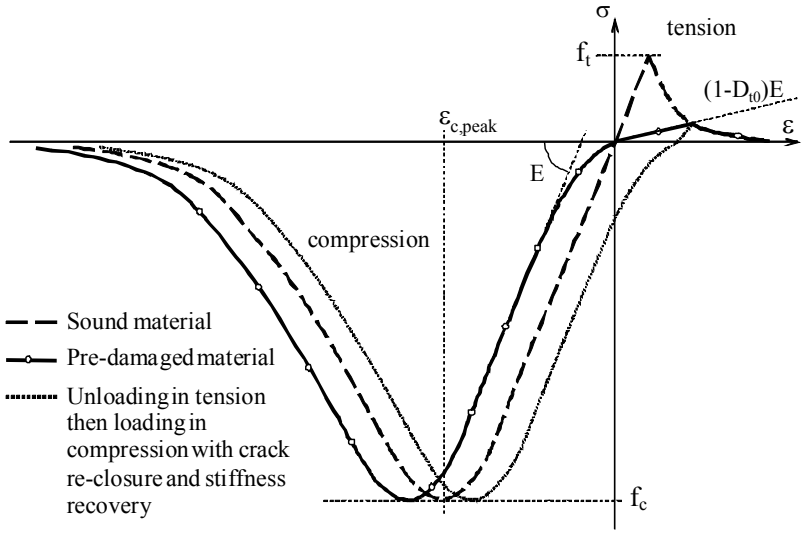

Fig. 1 Comparison between the sound material and the pre-damaged material

The model calculates 3 internal variable types (D_c, D_t, CMOD), useful to estimate the state of the structure. The calculation process determines the locations and the directions of the main cracks that develop, independently of the mesh.

2.3. Homogenization process in compression

In a macro approach, a homogenization law is used to represent the mechanical behaviour of the healthy masonry (without any crack or pre-damage). As it is, of course, not possible to remove a representative volume of the various components from the bridge masonry, a numerical homogenization process is performed to determine the mechanical parameters of the masonry behaviour law. The mechanical parameters of each component of the masonry (stones, mortar, and interface between joints and blocks) are determined separately, then introduced into a numerical calculation of a masonry elementary volume, as suggested in a previous study presented at SAHC 2010 (Domede [5]). The steps of the homogenization method can be summarized as follows:

- Experimental characterization of
  - The mortar and the stones by means of compressive tests,
  - The stone-mortar interface by means of 3-point bending tests,
- Fitting of the individual mortar and stone behaviour laws with the damage model,
- Numerical calculation of an elementary volume of masonry and fitting of the parameters of the homogenized masonry damage law used for the bridge calculation.

The representative elementary volume chosen is a numerical wall, the dimensions of which are defined in the European standard specifications (EN 1052-1, 1999). The wall is loaded by applying a vertical displacement inducing compression and transverse tensions in the composite wall.

3. THE BRIDGE STUDIED

3.1. Description of the current state of the bridge

The bridge studied (Figure 2) was a long stone masonry viaduct built in 1904 (9 spans, total length 136 m) in the close neighbourhood of Paris. Traffic on the two lines is very intense and the bridge supports the repeated passage of suburban passenger trains and freight trains, with 80 to 150 crossings daily.

Fig. 2 The masonry bridge studied (9 spans about 12.50 m long, 8 m wide). Archive plan 1904

On this bridge, disorders have appeared in the past: displacements of foundations, and transversal, longitudinal and skew cracks (Figure 3). Reinforcements have been made by adding steel arches under some arches of the viaduct. Concrete and steel micro-piles were installed beside the original timber piles in 2008. Cracks can be seen on the spandrel wall and in the intrados of the vaults. They appear in the mortar joints between the stone blocks (especially longitudinal and skew cracks under the intrados), and also through the stones themselves.

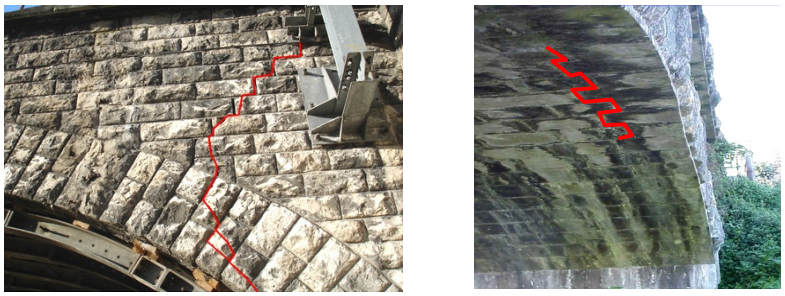

Fig. 3 Transversal crack in a spandrel wall (left) and longitudinal crack in the intrados (right)

3.2. Measurement of displacements and crack opening under service loads

All the measurements were made while a freight train was crossing the bridge. They included:

- Measurement of relative and absolute deflection under the intrados at mid span,
- Measurement of horizontal and vertical displacement at 4 points,
- Measurement of width of cracks (precision 10.10-6 m).

At the same time, train weight, temperature and relative humidity were noted.

3.3. Extraction of cores from the masonry elements

In July 2008 and January 2009, 5 cores were extracted from the bridge, in the third span, from under the intrados of the vault. The cores are 0.7 to 1.20 m long, with a diameter of 9.5 cm (Figure 4). Examination of the cores shows that 2 types of stone exist in this masonry bridge: a beige, exterior facing stone (at left on the photo) and another, grey stone for interior masonry (at right on the photo). The mortar that links the stone blocks consists of small and large aggregates. From these cores, small samples were extracted in each of the 3 components to determine their individual properties, and in the mortar above the mortar-block joints to determine its behaviour when embedded between two stone blocks. The behaviour of the mortar-stone interface was also investigated, as described later.

4. EXPERIMENTAL TESTS IN LABORATORY

4.1. Individual mechanical characteristics of stones and mortar

The mechanical parameters of each component of the masonries (stones, mortar, and mortar-stone interface) were determined separately by means of a 3-step experimental procedure. Following this experimental phase, the complete behaviour laws for mortar and stones were fitted with the damage model.

Step 1: individual experimental characterization of the mortar and the 2 stones
The two stones are calcareous, homogenous and isotropic. The characteristics given in Table 1 result from classical mechanical tests carried out in the laboratory (volume, mass and porosity according to EN1936, uniaxial compression tests as defined in EN1926 and EN14580, split tensile test with NFP94-422-5).

Table 1 Parameters used for individual materials

Material	**Poisson coefficient**	**E [GPa]**	**f_c [MPa]**	**G_{fc} [MJ/m^2]**	**$\varepsilon_{c,peak}$ [mm/m]**	**f_t [MPa]**	**G_{ft} [MJ/m^2]**
Interior stone	0.26	76 ±6%	172 ±8%	0.29	3.7	8 ±18%	7.10^{-4}
Facing stone	0.25	39 ±8%	120 ±3%	0.15	3.2	10 ±13%	2.10^{-4}
Mortar	0.19	5 ±1%	19 ±5%	0.02	2.8	1.2 ±17%	$0.25.10^{-4}$

Step 2: experimental characterization of the confinement effect of mortar
This was achieved by means of compression tests on stone-mortar-stone multilayers. Nine uniaxial compression tests were carried out on cylindrical cores (diameter 2.65 cm, height 6.6 cm to 9.25 cm) including mortar embedded between two pieces of stone (Figure 4). The failure of the sample resulted from failure of the mortar when the mortar width was large relative to that of the stone, but from failure of the stone (axial crack) when the mortar width was small, because of the confinement effect applied to the mortar joint by the bonded stone blocks.

Step 3: experimental characterization of the stone-mortar interface in tension
Six 3-point-bending tests were carried out on special samples made of a mortar joint embedded between 2 pieces of stone as can be seen on Figure 4 (displacement increasing by 0.01 mm/min). The parameters chosen for the mortar are given in Table 1.

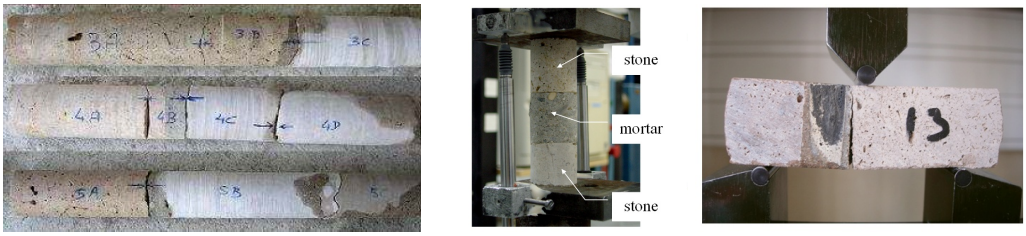

Fig. 4 Core compression tests (left) and 3 points-bending test on multilayers (right)

A numerical analysis of this test determined the confinement parameter $\delta = 0.52$ (relative to an internal friction angle $\varphi = 23°$).

4.2. Homogenization

The general principle adopted for the homogenization process was the following:

- In tension: the homogenized behaviour was that of the mortar-stone interface but with additional pre-damage to simulate the weakness of the mortar-block bond, as explained previously. The law adopted is shown in Figure 5. The pre-damage in tension D_{t0} was 0.9.
- In compression: the mortar and the stone behaviours were unified by calculating a representative elementary volume as explained in section 2.3. We obtained the parameters given in Table 2 (The stone blocks' dimensions were 40 cm × 20 cm × 30 cm. The mortar joint thickness was 2 cm).

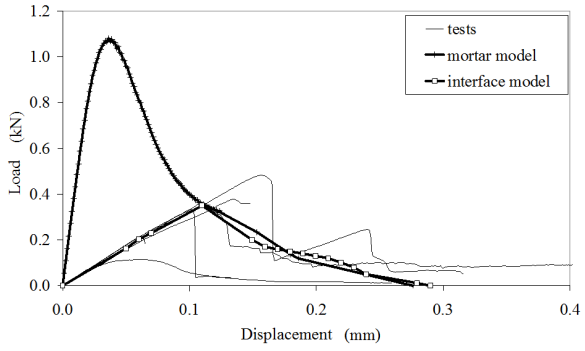

Fig. 5 Homogenized behaviour law in tension

Table 2 Parameters of homogenized behaviour law of masonries in compression

Masonry	Poisson coefficient	E [GPa]	f_c [MPa]	G_{fc} [MJ/m^2]	$\varepsilon_{c,peak}$ [mm/m]
Interior stone	0.25	41	116	0.37	3.7
Facing stone	0.25	27	84	0.23	3.6

No samples of the backfill were taken (coring too short). We assumed that the backfill acted as cohesive sand: it was modelled using a Drucker Prager criterion with a negligible cohesion and negligible tensile strength.

5. NUMERICAL ANALYSIS OF THE BRIDGE STUDIED

5.1. Mesh and boundary conditions

For numerical capacity reasons, only 3 spans were modelled with the model implemented in the FEM code Ansys. They were spans numbers 2, 3 and 4. The mesh was built in such a way that the final calculation tool could be used for any masonry arch. The bridge was divided into 5 zones (Figure 2, the piers are not modelled): the vault, embedded between the two spandrel walls and the two rings, the abutments and the backfill. The rails and the ballast were added on to the bridge (4 lines as can be seen on Figure 8), by means of 2D elements with an elastic linear law linked to the structure by joint elements (relative density = 1.7; E = 30 GPa; ν = 0.2; vertical rigidity = 100 MPa/m; longitudinal rigidity = 1000 MPa/m). The vertical planes located at each end of the three calculated spans were blocked horizontally in order to simulate the continuum of the bridge on each side, symmetrically. The soil and foundations under the bridge were modelled by means of elastic joint elements, the rigidity of which was calculated with respect to the results of on-site investigations (displacements of pile bases under freight train loads as described in 3.2). A first calculation of the bridge determined the foundation rigidity in such a way that the vertical displacement of the foundations under the freight train reached the mean value measured (0.22 mm).

5.2. Methodology and results of calculation

The bridge was calculated under 3 successive loadings: self-weight, foundation displacements, train.

Self-weight

Under self-weight, the vault deflection was 2.2 cm. A few cracks appeared symmetrically (Figure 6).

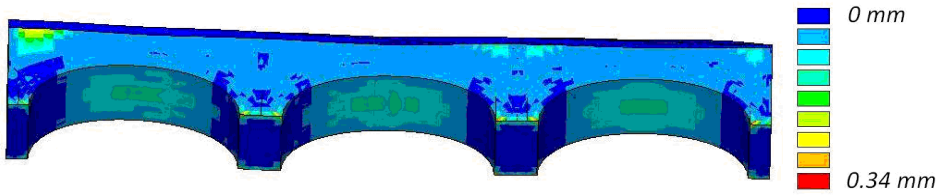

Fig. 6 CMOD and cracking scheme under self-weight

Displacements of foundations

In order to create a skew crack under the intrados of the third span, as actually observed, the following displacements were applied: 12 cm for one side, 5 cm for the other (Figure 7). Note that these imposed displacements were not measured on site, but fitted to explain the current crack pattern observed.

Train load

Finally, a train load was applied to the cracked bridge and was increased until collapse (The worst position of the train had been determined in advance by means of a simplified elastic calculation). The cracking scheme to collapse is given on Figure 8 and the load-displacement curve on Figure 9. The calculation was stopped at the peak load of 25 MN, i.e. a train load of 15 MN. We observed that the deflection calculated under service load was about 1 mm, i.e. three times those measured (about 0.3 mm). We think that the parameters introduced in the crack re-closure function could be improved. This is feature that needs further study considering the real deflection of the bridge under service load.

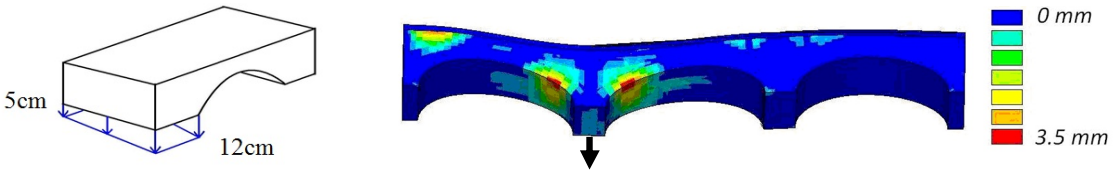

Fig. 7 Displacements of foundations to create the initial cracked state, and CMOD

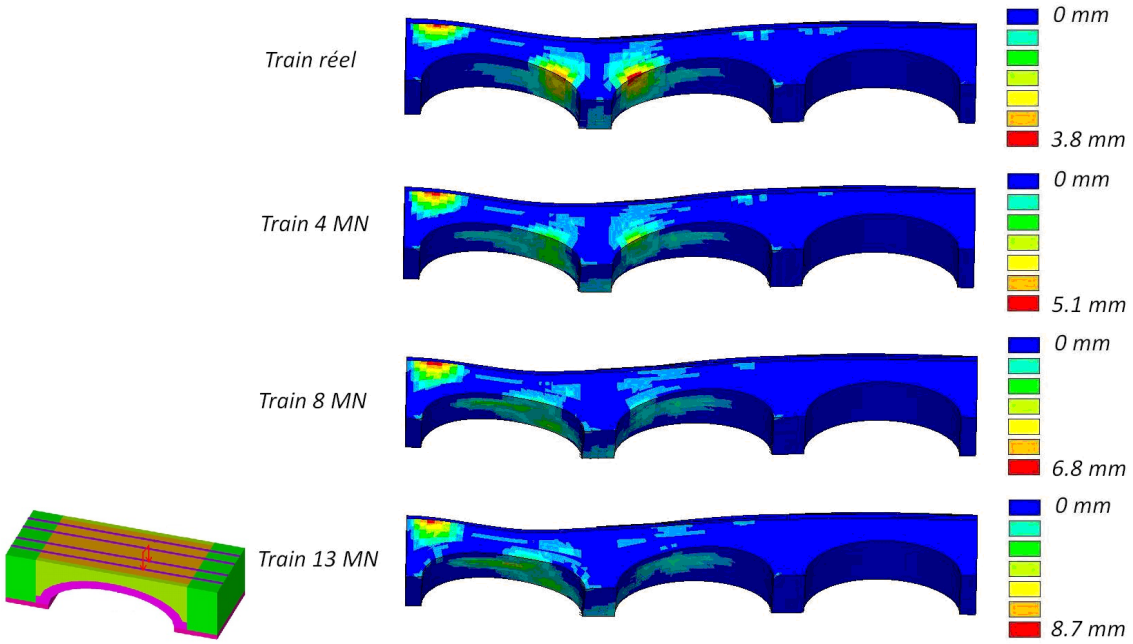

Fig. 8 CMOD and cracking scheme under train load

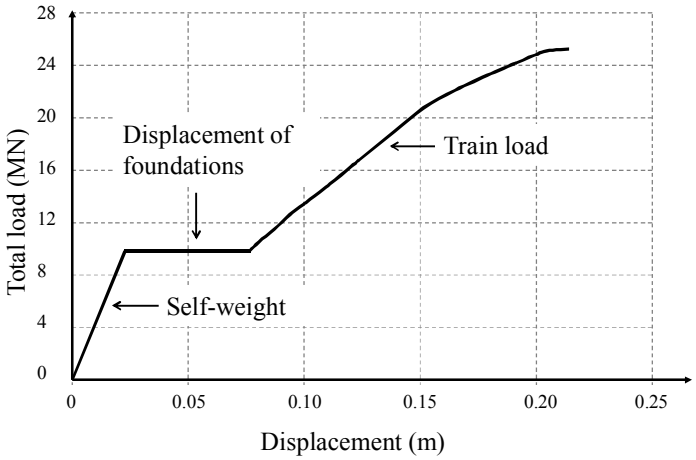

Fig. 9 Position of the axle load (left) and deflection of the vault under train load until collapse (right)

6. CONCLUSIONS

A global methodology has been proposed to assess masonry bridge behaviour. It is based on a numerical model able to describe the crack pattern and to consider the initial damage in the homogenized material. The implementation of the model in a 3D FE code allows the whole history of the structure to be simulated from its construction onwards. An important step in the method is to observe the current cracked state of the bridge, considered as the initial state of the calculation under traffic load. For that, just after applying the self-weight, a foundations displacement field is determined in order to obtain compatibility between the on-site crack pattern and the numeric response. The calculation of the bridge under loads is carried out until collapse. Finally, the calculation results provide a realistic description of the masonry behaviour in terms of cracking, and give interesting information for practitioners: crack opening under passage of a freight train, pile movements and, of course, maximal loading to assess the safety level.

ACKNOWLEDGEMENTS

The financial support by the SNCF and RFF granted to the LMDC laboratory for this research is gratefully acknowledged.

REFERENCES

[1] Orban Z., UIC. (2005) Improving assessment optimization of maintenance and development of database for masonry arch bridges, Progress report.
[2] Proske, D. Van Gerlder, P. (2009) *Safety of historical stone arch bridges*, Springer.
[3] Roca, P., Cervera M., Gariup G., Pela L. (2010) Structural analysis of masonry historical constructions. Classical and advanced approaches, *Archives of Computational Methods in Engineering* 17:299-325.
[4] Sellier A., Bary B. (2002) Coupled damage tensors and weakest link theory for describing crack induced orthotropy in concrete, *Engineering Fracture Mechanics* 1629.
[5] Domède N., Sellier A. (2012) Experimental and numerical analysis of behaviour of old brick masonries, In: *Proc. Int. Conf. SAHC 2010,* Shangai, China.
[6] Stablon T. (2011) *Méthodologie pour la requalification des ponts en maçonnerie*, PhD thesis, Université de Toulouse.
[7] Erdogan F., Sih G.C. (1963) On the crack extension in plates under plane loading and transverse shear, *Journal of Basic engineering*, 85:519-527.
[8] Stablon T., Sellier A., Domede N., Plu B., Dieleman L. (2011) Influence of building process on stiffness: numerical analysis of a masonry vault including mortar joint shrinkage and crack re-closure effect, *Materials and Structure*.